Exploiting the effects of mass transfer to boost the performances of Co/γ-Al2O3 eggshell catalysts for the Fischer–Tropsch synthesis

Laura Fratalocchi [a], Carlo Giorgio Visconti [a,*], Luca Lietti [a,*], Enrico Tronconi [a], Stefano Rossini [b]

[a] Politecnico di Milano, Dipartimento di Energia, Via La Masa, 34-20156 Milano, Italy
[b] Eni S.p.A., Via Maritano, 26-20097 San Donato Milanese Italy

In this work, the performances of a spherical Co/□-Al2O3 eggshell catalyst characterized by a diameter of 600 □m and an active shell region 75 □ m thick are assessed in a lab-scale fixed bed reactor operated at industrially relevant Fischer–Tropsch process conditions. Such performances are compared to those of a powder catalyst obtained by grinding and sieving a fraction of the eggshell catalyst so to obtain powders with a particle size distribution centered in the range 75–100 □m. It is shown that, thanks to the presence of modest mass transport restrictions, the eggshell catalyst outperforms the corresponding powder in terms of C15+ specific yield. We explain these results by considering the effect of mass transport on the olefin re-adsorption probability and on the H2/CO ratio in proximity to the active sites. The former is increased, and results in greater selectivity to heavy hydrocarbons. The latter is also increased, due to the negative order of CO conversion kinetics with respect to CO, and results in augmented reaction rate.

Keywords: Eggshell catalysts, Fischer–Tropsch synthesis, Compact fixed-bed reactors, Weak mass transfer limitations

1. Introduction

The low temperature Fischer–Tropsch (LTFT) synthesis aims at converting synthesis gas, the mixture of carbon monoxide and hydrogen derived from natural gas, coal, biomass or waste, into long-chain hydrocarbons. The process is carried out at temperatures below 250 °C and pressures over 20 bar in the presence of a heterogeneous catalyst. The catalysts used at the industrial scale are based on cobalt and iron [1], usually promoted with other elements such as noble metals or potassium. Cobalt is usually adopted for gas to liquid (GTL) applications, while iron is used in coal, biomass and waste to liquid (CTL, BTL, WTL) plants. Indeed, when the H_2/CO ratio in the available syngas is close to the stoichiometric value (∼2), such as in GTL applications, Co-based catalysts supported on high surface area oxides are preferred for their greater intrinsic activity, higher selectivity to linear long-chain paraffins, and negligible water-gas shift activity. On the contrary, for H_2-deficient syngas, like in CTL, BTL and WTL applications, iron based catalysts are preferred because their intrinsic water-gas-shift activity allows to increase the H_2/CO ratio in the reactor.

The Fischer–Tropsch synthesis (FTS) is a surface-catalyzed polymerization involving the chain growth monomer CH_2^* and growing alkyl species [2]. The stepwise addition of C_1 monomer to a surface alkyl may terminate by adding or eliminating a hydrogen atom to the growing species, which hence desorbs as paraffin or α-olefin, respectively [3,4]. While the former species is terminal, the α-olefin may re-adsorb on the catalytically active sites and give secondary reactions including the hydrogenation to the corresponding paraffin, the chain growth or the reaction with a CO molecule to form an oxy-species. The occurrence of secondary reactions depends on the olefin diffusion rate within the pores of the pellets, which are full of liquid hydrocarbons at typical Fischer–Tropsch (FT) process conditions [5,6]. The slower is the olefin diffusion, the higher is the probability for an olefin to be readsorbed and undergo secondary reactions. This is the reason why the olefin to paraffin ratio (O/P) in the Fischer–Tropsch product decreases upon increasing the carbon number. Also, the occurrence of secondary reactions is a function of the characteristic length of intraporous diffusion, i.e., of the size of the catalyst pellet. The higher this is, the greater is the possibility for the secondary reaction of olefins to occur.

Although CO and H_2 diffusion rates are much faster than those of olefins, it has been reported that the FT activity and selectivity may be also affected by their diffusion rate within the pores of the pellets. Indeed, hydrogen molecular diffusivity in the liquid waxes is twice as high as that of carbon monoxide [7]. Accordingly, in the

* Corresponding authors. Fax: +39 02 2399 8566.
E-mail addresses: carlo.visconti@polimi.it (C.G. Visconti), luca.lietti@polimi.it (L. Lietti).

Published Journal Article available at: http://dx.doi.org/10.1016/j.apcata.2015.12.011

presence of strong mass transfer limitations, the local H_2/CO ratio in close proximity of the catalyst active centers may be significantly higher than in the bulk phase.

A comprehensive review paper by Iglesia et al. [2] discusses the effect of the characteristic length of diffusion (δ) on the LTFT reactivity. By comparing the performances of Co/SiO_2 spherical catalysts with different diameters (from 130 to 1500 μm), the authors observe that by increasing the pellet size, the selectivity to C_{5+} goes through a maximum, achieved in correspondence of a pellet size of 360 μm ($\delta = 60$ μm). According to their interpretation, the C_{5+} selectivity initially increases as a result of the favored α-olefins readsorption, which results in increased chain growth probability. Ultimately, however, larger pellets become depleted of CO (i.e., rich in H_2), leading to enhanced hydrogenation reactions and hence to a decreased C_{5+} selectivity. For the same reason, increasing pellet diameter until 360 μm lowers the selectivity to methane; then, for bigger pellets, the methane selectivity increases with growing pellet size. Interestingly, the authors notice that the olefin content in FT products decreases monotonically on increasing the pellet size. The initial decrease of olefins is explained by considering their enhanced readsorption. Then, the unsaturation of the products further decreases because of the combined effect of the longer intrapellet "residence time" of the olefins and the higher H_2 concentration near catalytic sites.

Surprisingly, although marked selectivity changes occur by increasing the pellet size, the authors note that the FT rate, expressed as cobalt time yield, is not influenced by the pellet size [2].

The effect of the catalyst pellet size on FT catalytic performances has been also studied by Post et al. [8], working with both iron and cobalt supported catalysts. In partial disagreement with the results shown in [2], these authors show that upon decreasing the pellet diameter from 2 mm ($\delta = 333$ μm) to less than 1 mm ($\delta \leq 166$ μm) both the synthesis gas conversion and the catalyst productivity (expressed as space time yield, $kg_{C1+}/m^3{}_{cat}/h$) increase.

The effect of the average diffusion length on FT catalyst performances has been also studied on structured monolithic catalysts by varying the thickness ($t = \delta$) of the washcoated catalytic layer [9,10]. In these works it is shown that diffusive lengths below 50 μm are exempt from diffusive limitations, while monoliths with thicker washcoats suffer from internal diffusion limitations which cause lower CO conversion rates and lower C_{5+} selectivities [9,10].

In summary, even though the real effects of "weak" mass transfer restrictions on the catalyst activity and selectivity are not clear so far, there is a general consensus on the fact that in order to avoid the onset of mass transport limitations, it is important not to exceed the diffusion characteristic length of 50–60 μm [2,10]. This requires to operate with monolithic honeycombs washcoated with thin active layers (50–60 μm thick) or with small evenly impregnated pellets (with diameters of 300–360 μm if spherical). This catalyst size is unsuitable to be applied in industrial fixed-bed reactors. Indeed, packed beds would suffer of unacceptable pressure drops, while structured reactors would be limited by the insufficient catalyst inventory [11,12]. In fixed bed reactors, a smart solution to prevent the onset of strong mass transfer limitations while granting low pressure drops at the same time is represented by eggshell-type supported catalysts [13–19]. Such catalysts are characterized by the presence of the active phase only in the peripheral region of the pellet, which is referred to as "active shell". In this way, the pellet diameter and the diffusion characteristic length become two decoupled parameters, which can be optimized independently. Indeed δ does not correspond anymore to one sixth of the pellet diameter (as in the case of evenly impregnated spherical pellets), but is calculated by using the following Eq. (1), where t, V and S are the active shell thickness, volume and outer surface, respectively, and R is the pellet radius [19]:

$$\delta = \left(\frac{V}{S}\right)_{shell} = \frac{\frac{4}{3}\pi\left(R^3 - (R-t)^3\right)}{4\pi R^2} = \frac{\left(R^3 - (R-t)^3\right)}{3R^2} \quad (1)$$

The development of compact FT reactors, which are particularly interesting for stranded and off-shore GTL applications, or for BTL (biomass-to-liquid) plants, led, in the last decade, to look for intensified reactor technologies. As a result, microchannel and structured fixed-bed reactors [20–23] with improved heat transfer performances have been proposed. In order to make such technologies economically sustainable, these reactors have to grant high productivity per unit catalyst volume. Accordingly, the development of catalysts with exceptional level of activity, but not limited by strong mass transfer restrictions, is mandatory. In this perspective, the development of eggshell pellets with diameter below 1 mm is of particular interest.

In a recent work by some of us [19], a new procedure to prepare "small" eggshell $Co/\gamma\text{-}Al_2O_3$ catalysts (with diameters as low as 600 μm) suitable for compact Fischer–Tropsch reactors has been proposed. By using a new impregnation method based (i) on the "protection" of the support pores with an organic solvent, (ii) on the adoption of a polar impregnating solution containing the catalyst precursor, and (iii) on the contact of the support with the precursor solution for a controlled time, we have shown that eggshell catalysts with a diameter as low as 600 μm, impregnated with 16 wt.% cobalt in a thin external region as thin as 75 μm, can be prepared. The diffusive length of this eggshell catalyst, calculated by Eq. (1), is 58 μm. In this work, in order to gain more insight in the effects of the characteristic length of diffusion, and to verify the possibility to enhance the performances of a $Co/\gamma\text{-}Al_2O_3$ catalyst by taking advantages from the consequences (i.e., the increased C_{5+} selectivity and CO conversion rate) of weak mass transfer restrictions, the performances of such an eggshell catalyst have been assessed, and compared to those of a powdered sample working in a kinetically controlled regime.

2. Experimental

Eggshell catalysts have been prepared by adopting the procedure reported in our previous paper [19], whose main steps are listed in the following. At first, $\gamma\text{-}Al_2O_3$ microspheres (Sasol Puralox®, $S_{BET} = 161\ m^2\ g^{-1}$, $V_{pore} = 0.41\ cm^3\ g^{-1}$, $D_{pellet} = 600$ μm) have been soaked in *n*-undecane (Sigma–Aldrich, 99 wt.%) for 40 min; then, they have been drained from the excess hydrocarbon and placed into a fritted glass funnel mounted on a vacuum flask. At this point, the impregnating solution, constituted by $Co(NO_3)_2{\cdot}6H_2O$ (Sigma–Aldrich, 98 wt.%) in ethanol (Carlo Erba, 97 wt.%; $1.27\ ml_{ethanol}/g_{salt}$), has been poured onto the spheres ($5.6\ ml_{solution}/g_{Al2O3}$) and, after 2 s, the excess solution has been rapidly removed from the funnel by evacuating the flask. Eventually, the impregnated spheres have been dried in static air at 393 K for 2 h and then calcined at 673 K in static air for 12 h. By repeating nine times the procedure, eggshell pellets with a diameter of 600 μm (namely ES600) and with a Co loading in the active shell of 16 wt.%, corresponding to a Co loading of 9.3 wt.% calculated considering also the weight of the non-impregnated core, have been obtained. As shown in Fig. 1(a), those samples are characterized by a sharp and homogeneous shell layer 75 μm thick ($\delta = 58$ μm).

The eggshell catalyst has a BET surface area of $143\ m^2\ g^{-1}$ and a pore volume of $0.27\ cm^3\ g^{-1}$, corresponding to an average pore diameter of 7.5 nm. The average Co_3O_4 crystallite diameter (d_{cry}) is 6.8 nm, from which an average Co^0 crystallite size of 5.1 nm can be determined [24]. This value is close to the ideal crystallite size granting the maximum active phase dispersion, without entering in

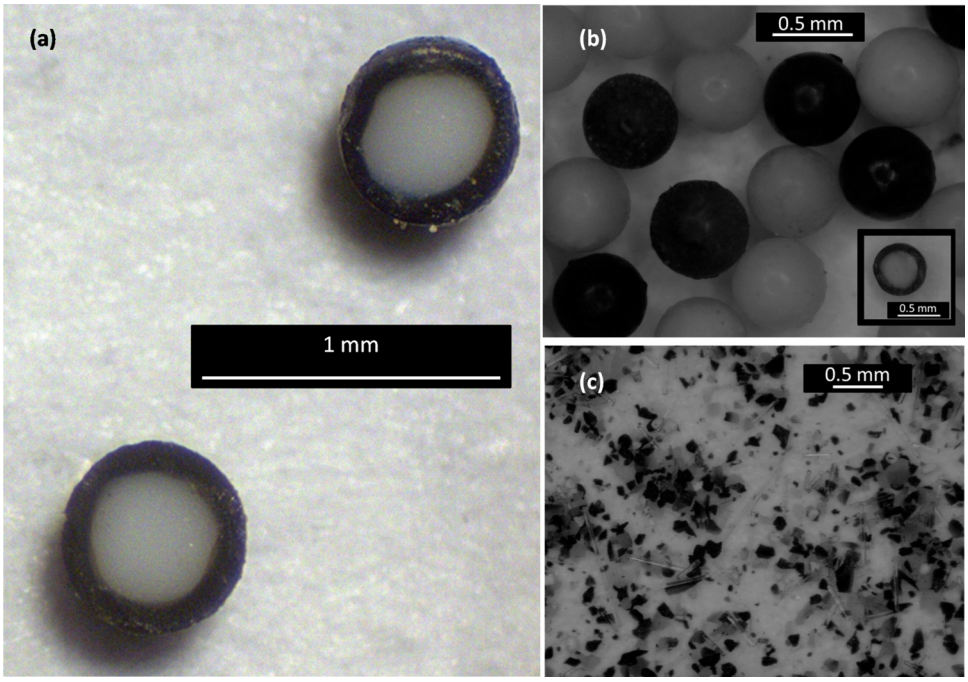

Fig. 1. Optical micrographs of the (a) fresh ES600 sample (section) and of the used (b) ES600 (section in the inset) and (c) POW100 catalysts.

the area (d_{cry} < 6–8 nm [25]) where the Fischer–Tropsch synthesis becomes a structure sensitive reaction.

A fraction of the eggshell catalysts has been ground and sieved with a sieve having 150 μm opening so to obtain a powdered sample with the same chemico-physical properties of the unground eggshell sample with the exception of the characteristic length of diffusion. Indeed, in order to guarantee that the powdered sample had the same composition as the eggshell sample, grinding and sieving processes have been prosecuted until the eggshell catalyst has been entirely ground in powders below 150 μm.

In order to estimate the average size and shape of the powdered particles, as well as to verify the integrity of the eggshell catalyst after catalytic tests, microscopy analyses have been performed on the used catalysts. To the scope, an optical microscope (Stereo Discovery V12) and an image analysis software (Image-J) have been used. Eventually, the approximate sphericity of the powdered particles has been estimated by applying the correlations reported in Supplementary material.

Fischer–Tropsch activity tests have been carried out with both the egg-shell and the powdered sample operating in a lab-scale tubular packed reactor (1.1 cm I.D., 85 cm long) with plug-flow hydrodynamics (Fig. S2). A sketch and a description of the adopted lab-scale setup can be found elsewhere [26]. In order to prevent axial temperature gradients caused by the strongly exothermic FTS, adopted eggshell and powdered catalysts have been diluted with α-Al_2O_3 micro-spheres with 600 and 100 μm, respectively, so to obtain beds 11 cm long.

Prior to the activity tests both the catalysts have been reduced in situ by feeding 35.95 L(STP) $h^{-1}g_{Co}{}^{-1}$ of H_2 (Sapio, 99.995 mol.%) and keeping the catalyst at 400 °C (heating ramp from ambient temperature to 400 °C at 2 °C/min) for 17 h. This procedure allows to achieve an extent of reduction in the range 55–67% [19], which is a value higher than those reported in the literature for similar un-promoted Co/γ-Al_2O_3 catalysts, suggesting an excellent reducibility of the adopted samples [27]. After this treatment, catalytic runs have been performed at process conditions relevant to industrial operations: T = 220–230–240 °C, P = 25 bar, H_2/CO inlet molar ratio = 1.7, GHSV = 46.01 L(STP) $h^{-1}g_{Co}{}^{-1}$, N_2 + Ar in the feed = 24 vol.%. Each time we changed the process conditions, we collected data until steady-state conditions were reached both in terms of CO conversion and product selectivity. This required to operate the catalyst in each investigated condition for more than 100 consecutive hours. Reactants and C_1–C_{49} products (paraffins, olefins and alcohols) leaving the reactor have been quantified by on-line and off-line gas-chromatography. The details on the products collection and on the GC analyses can be found elsewhere [26]. Carbon balances, calculated as moles of C contained in the reaction products divided by the moles of converted CO, always closed within ±5%.

3. Results and discussions

3.1. Working catalyst characterization

Fig. 1(b and c) shows the optical micrographs of the used catalysts, which we assume to be representative of the working catalyst. In addition to the catalytic material, residues of quartz wool fibers, used as inert filling of the reactor (more details on the reactor loading scheme can be found in Supplementary material), and α-Al_2O_3 spheres, used as diluent of the catalytic bed, are also present.

Fig. 1(a and b) shows that the particle size, the particle shape and the "eggshell-type" configuration of the used eggshell sample is unchanged even after several hours on stream. This indicates high mechanical strength and chemical resistance of the eggshell pellets, which is a fundamental property for catalysts to be used in packed bed reactors.

Fig. 1(c) shows that the particles shape of the powdered catalyst is irregular and that different types of particles exist: (i) grey particles entirely constituted by γ-Al_2O_3 (possibly obtained by fragmentation of the inert core of the eggshell catalyst), (ii) black particles entirely constituted by Co/γ-Al_2O_3 catalyst (active shell), and (iii) black and grey particles constituted by a fraction of γ-Al_2O_3 and a fraction of Co/γ-Al_2O_3. The average size of the crushed eggshell catalyst, estimated by measuring the maximum and the minimum dimensions of about two-hundred of these particles, results centered in the range 75–100 μm. Accordingly, the

Table 1
POW100 catalyst stability $T = 230\,^{\circ}C$, $P = 25$ bar, $H_2/CO = 1.7$ mol/mol and GHSV = 46.01 L(STP) $h^{-1} g_{Co}^{-1}$, inerts (N_2+Ar) in the feed = 24 vol.%.

T.o.S. [h]	X_{CO}[%]	S_{CH4} [%]	S_{C5+}[%]
44	34.2	10.7	74.1
66	33.6	11	72.7
87	33.7	11	73.2
161	34.1	10.9	73.3
656	33.7	10.9	73.1

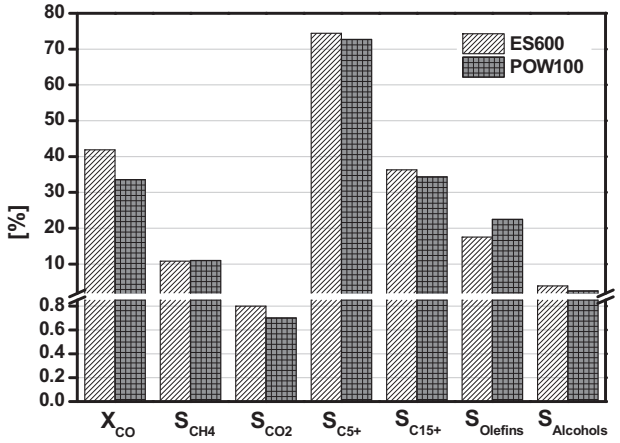

Fig. 2. CO conversion (X_{CO}) and selectivity (S) to the main reaction products. P.C.: $T = 230\,^{\circ}C$; $P = 25$ bar; H_2/CO inlet molar ratio = 1.7; GHSV = 46.01 L(STP) $h^{-1} g_{Co}^{-1}$; inerts (N_2+Ar) in the feed = 24 vol.%; $T.o.S.^{ES600} = 70$ h and $T.o.S.^{POW100} = 87$ h.

powdered sample has been named POW100. The average sphericity of POW100 particles, calculated as the average ratio between the surface area of an ideal sphere with the same volume as the given particle, and the surface area of the particle, is 0.78–0.79. The corresponding diffusive length, calculated as shown in the Supplementary material, is below 20 μm, a value assuring operations under kinetically control regime [2,10].

3.2. Catalysts stability

In order to collect representative steady-state activity data, both the catalysts considered in this work have been tested for more than 700 h. In spite of the long runs, as already seen in the case of the eggshell catalyst [19], also the powdered catalyst has been found to be very stable with the Time on Stream (T.o.S.) both in terms of activity and selectivity (Table 1). In particular, CO conversion varies from 34.2% at T.o.S. 44 h to 33.7% at T.o.S. 656 h while CH_4 and C_{5+} selectivities vary from 10.7 and 74.1% at T.o.S. 44 h to 10.9 and 73.1% at T.o.S. 656 h.

3.3. Catalysts activity and selectivity

Fig. 2 shows the steady-state CO conversions measured at 230 °C, 25 bar, H_2/CO feed molar ratio = 1.7, GHSV = 46.01 L(STP) $h^{-1} g_{Co}^{-1}$, inerts in the feed = 24 vol.%, over the eggshell (ES600) and the powdered eggshell (POW100) catalysts measured respectively at T.o.S. 70 and 87 h. The selectivities to methane, carbon dioxide, C_{5+} and C_{15+} hydrocarbons, olefins and alcohols are also shown.

The ES600 catalyst is more active than POW100, as demonstrated by a CO conversion of 42% versus a value of 34% measured over the POW100 catalyst. In terms of FT products selectivity, the two catalysts show similar selectivity to methane (~11.0%) and carbon dioxide (<1.0%). The C_{5+} and C_{15+} selectivities are also very similar for the two catalysts, with ES600 only slightly more selective to heavier species than POW100 ($S_{C5+}^{ES600} = 74\%$, $S_{C15+}^{ES600} = 36\%$, $S_{C5+}^{POW100} = 73\%$, $S_{C15+}^{POW100} = 34\%$). As a result, the Anderson–Schulz-Flory (ASF) plots obtained for the two catalysts (Fig. 3) show similar hydrocarbon distributions with the typical positive and negative deviations for methane and C_2 hydrocarbons, respectively, and a change of slope for a carbon number around 8. The chain growth probability, estimated by considering the hydrocarbons with more than 15 carbon atoms (α_{C15+}), is close to 0.87 for both catalysts.

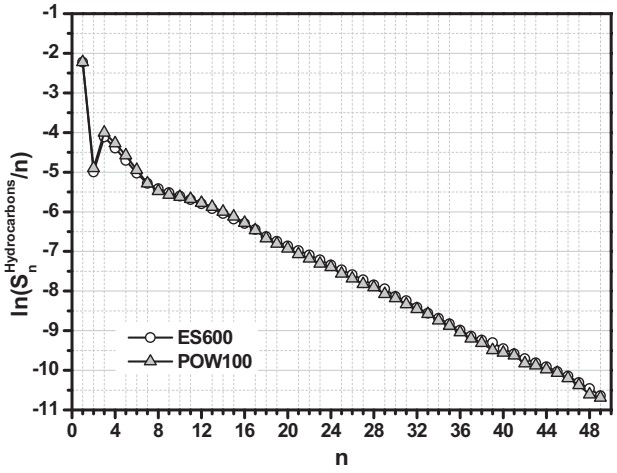

Fig. 3. ASF hydrocarbons distribution as a function of the carbon number. Process condition and T.o.S. as in Fig. 2.

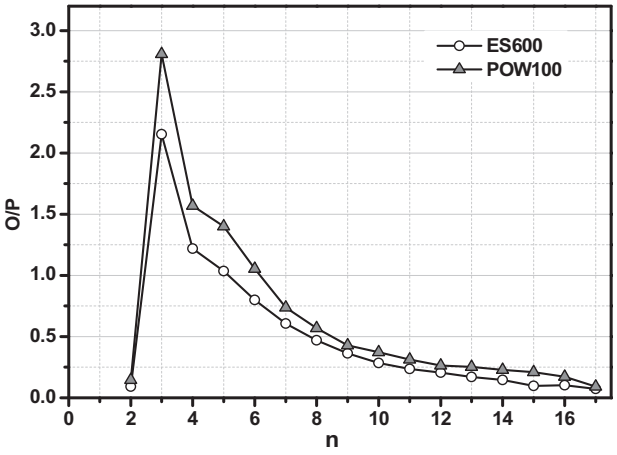

Fig. 4. Experimental olefin to paraffin ratio as a function of the carbon number. Process condition and T.o.S. as in Fig. 2.

On the other hand, the eggshell catalyst shows lower selectivity to olefins with respect to the powdered sample (18 vs. 23%), and slightly higher selectivity to alcohols (3.9 vs. 2.5%). As shown in Fig. 4, indeed, the olefin to paraffin ratio (O/P) plotted as a function of the carbon number (n) shows for both the catalysts the well-known monotonically decreasing distribution for $n > 2$, with ethylene out of trend, but POW100 shows higher O/P ratio than ES600, due to higher olefins selectivity together with lower paraffin selectivity (Fig. 5).

With both catalysts, the ASF diagram of alcohols (Fig. 6) shows distributions characterized by change of slope in correspondence of the C_4 species. As discussed elsewhere [28], such a peculiar trend can be explained by considering the presence of two different routes for alcohol formation, i.e. an independent chain growth route with oxy-species as intermediates (dominant for C_1–C_3 alcohols) and the hydroformylation of adsorbed olefins (dominant for

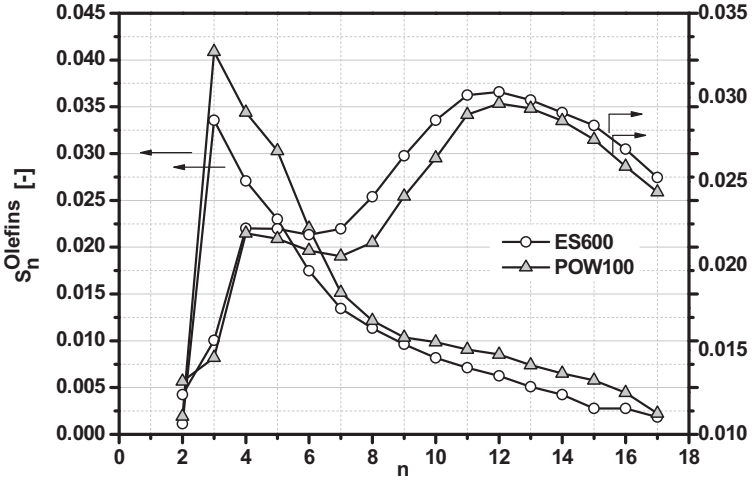

Fig. 5. Olefins and paraffins selectivities as a function of the carbon number. Process condition and T.o.S. as in Fig. 2.

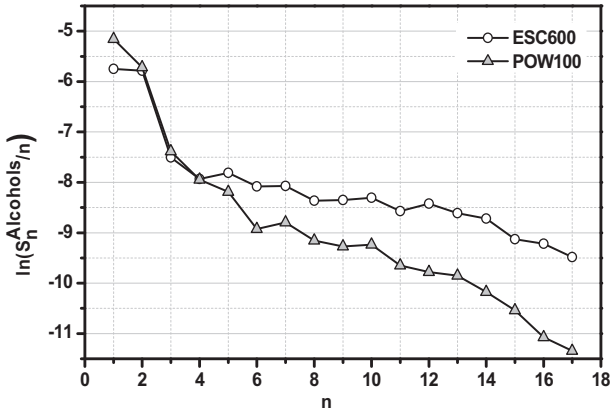

Fig. 6. Alcohols ASF distribution as a function of the carbon number. Process condition and T.o.S. as in Fig. 2.

C_4–C_{17} alcohols). Interestingly, ES600 and POW100 catalysts show similar C_1–C_3 alcohols selectivities, while for C_{4+} species the powdered sample shows lower selectivity to alcohols than the eggshell catalyst.

Such results may be explained by considering the different diffusion lengths of the eggshell (58 μm) and the powdered catalysts (≤20 μm). In particular, we speculate that the performances of the eggshell catalyst are influenced by weak mass transport limitations. In these conditions, indeed, we expect that the slow olefins removal results in increased readsorption probability. As a matter of fact, our data show that the products of the ES600 catalyst are less olefinic than those of POW100 (Fig. 4). Also, our data show that olefins readsorption is mainly followed by their hydrogenation to the corresponding paraffins (Fig. 5) and only a minor amount of readsorbed olefins is re-inserted in the chain growth mechanism. This result, evidenced by the slightly higher selectivity to C_{15+} of the eggshell catalysts with respect to the powdered sample (Fig. 2), is in good agreement by the results obtained by Fiore et al. [28] during olefin cofeeding experiments. The readsorbed olefins also undergo hydroformylation to the C_{n+1} alcohol ($n > 3$), as shown by the higher alcohols selectivity of the ES600 catalyst (Fig. 6), again in agreement with Fiore et al. [28].

Eventually, our data point out a CO conversion increase in the presence of weak mass transfer limitations. We explain such increase by considering that Fischer–Tropsch kinetics are positive order with respect to H_2 and negative order with respect to CO

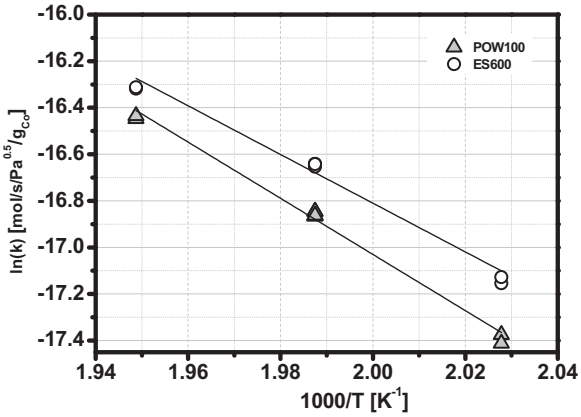

Fig. 7. Arrhenius plots for ES600 and POW100 catalysts.

[29] and that the different molecular diffusivities of H_2 and CO in the liquid waxes filling the catalyst pores [7] result in H_2/CO ratios higher in close proximity of the catalyst active centers than in the bulk phase.

Indeed, as typical of reactions with kinetics having negative dependencies on the concentration of the limiting reactant, there is a range of Thiele modulus (ϕ) centered around $\phi = 1$ where the effectiveness factor becomes greater than one [30]. Preliminary estimates of Thiele modulus, carried out using relevant literature intrinsic kinetics as well as literature data for CO diffusivity and solubility in the liquid phase, are in line with this scenario, providing values of ϕ between 1 and 1.5 depending on the reaction temperature.

3.4. Temperature effect and apparent activation energy

In order to confirm our speculation on the occurrence of "weak" mass transfer limitation for the ES600 sample, activity tests at different temperatures (220, 230, 240 °C) have been carried out on both ES600 and POW100 catalysts and their apparent activation energies have been estimated by using a literature power-law rate expression to describe the CO consumption kinetics [31]. In Fig. 7, the Arrhenius plots for the two catalysts are shown: they confirm the higher activity of ES600. In line with our explanation for the observed data, while an apparent activation energy of 100 kJ/mol has been estimated for the powdered sample, a value as low as 87 kJ/mol has been calculated for the eggshell catalyst. This shows that the presence of slight mass transfer restrictions falsifies the CO consumption kinetics on the eggshell samples.

A further confirmation of the presence of weak mass transfer limitations for the eggshell sample can be found by looking at the evolution with temperature of the product distributions of the two catalysts. Activity tests conducted at 220 °C confirm the results already obtained at 230 °C (Figs. 8 and 9). The presence of weak mass transfer limitations in the eggshell sample positively affects both the CO conversion kinetics and the catalyst selectivity. The hydrogenation of readsorbed olefins to the corresponding paraffins is still dominant on both the re-insertion in the chain growth mechanism and the hydroformylation to the C_{n+1} alcohol. More interesting are the results obtained at 240 °C. As shown in Fig. 8, the differences in the C_{15+} selectivity of the two catalysts become more evident, as pointed out also by the different values of the chain growth probability (α_{C15+}) estimated for both catalysts: 0.86 for POW100 sample and 0.87 for ES600 catalysts. Also the decrease of the O/P ratio is more marked at 240 °C than that recorded at 220 and 230 °C. Such results not only confirm that, as expected, the increase of temperature enhances the effects of mass transfer limitations, but also constitutes an additional proof that the reason

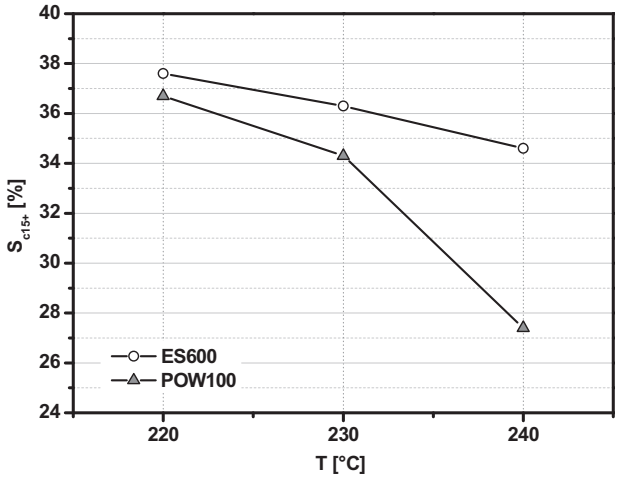

Fig. 8. Selectivity to C_{15+} hydrocarbons as a function of temperature. P.C.: T = 220; 230; 240 °C; P = 25 bar; H_2/CO inlet molar ratio = 1.7; GHSV = 46.01 L(STP) $h^{-1} g_{Co}^{-1}$; inerts (N_2+Ar) in the feed = 24 vol.% T.o.S.^{ES600}(230 °C) = 70 h, T.o.S.^{ES600}(220 °C) = 170 h, T.o.S.^{ES600}(240 °C) = 238 h and T.o.S.^{POW100}(230 °C) = 87 h, T.o.S.^{POW100}(220 °C) = 209 h, T.o.S.^{POW100}(240 °C) = 257 h.

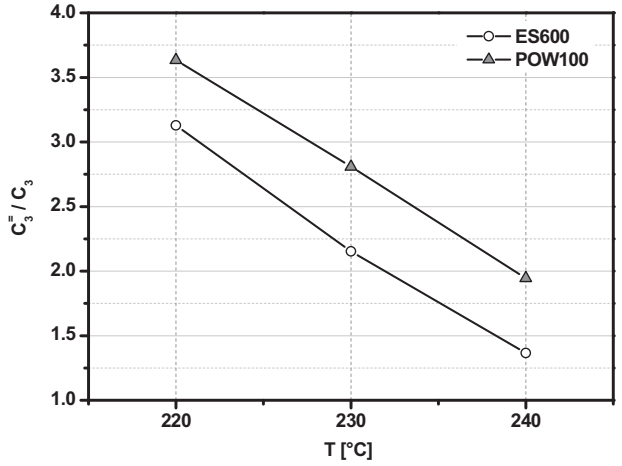

Fig. 9. Propylene to propane ratio as a function of temperature. Process condition and T.o.S. as in Fig. 8.

for the different selectivity of the two catalysts is the presence of intraporous mass transfer restrictions in the eggshell sample.

Notably, the presence of weak mass transfer limitations makes the performances of the ES600 sample better than those of the powdered sample, which operates under a kinetically controlled regime. Indeed, our data show that those restrictions boost the CO conversion kinetics (major effect) and increase the S_{C5+} selectivity (minor effect). This results in a C_{5+} yield (per g_{Co}) for the eggshell sample that is 29% higher than for the powdered sample. Such increased yield can be used at the industrial scale to compensate (at least partially) the lower inventory of active phase in the reactor (and consequently the lower C_{5+} yield per unit volume) which is obtained when an eggshell catalyst replaces an evenly impregnated sample.

4. Conclusions

Following the innovative preparation procedure recently developed in our group [19], a small Co/γ-Al_2O_3 eggshell catalyst with a diameter of 600 μm, a cobalt loading in the shell of 16 wt.%, a uniform thickness of the active shell and a diffusive length of 58 μm, has been prepared. Its catalytic performances in the Fischer–Tropsch synthesis have been compared to those of a powdered catalyst with a diffusive length below 20 μm, obtained by grinding and sieving the eggshell catalyst.

Interestingly, the eggshell catalyst shows higher CO conversion and C_{5+} selectivity with respect to the powdered sample. Also, the products are less olefinic than with the powder sample. We have explained these results by considering the occurrence of modest transport limitations in the case of eggshell catalyst, which boost both the CO conversion kinetics and the catalyst hydrogenating ability. The CO conversion is increased because the local H_2/CO ratio in close proximity of the active centers is higher than in the bulk phase, and the CO conversion kinetics are positive order with respect to H_2 and negative order with respect to CO. The slightly higher selectivity to heavy species and the lower content of olefins are related instead to the fact that the greater diffusion length of the eggshell catalyst enhances the probability of primary α-olefins to be re-adsorbed and hence to undergo secondary reactions. Among these, hydrogenation to the corresponding paraffin is dominant, even though minor increases of the chain growth probability and of hydroformylation to the C_{n+1} alcohol are also observed. As a confirmation to our explanation for the observed data, while the apparent FT activation energy for the powder catalyst is 100 kJ/mol, that estimated for the eggshell catalyst is as low as 87 kJ/mol.

From a fundamental point of view, our data prove that the onset of mass transfer restrictions in the LTFT affects both the catalyst activity and its selectivity. In particular, weak mass transfer limitations significantly boost the CO consumption kinetics, lower the olefinicity of the products and slightly increase the selectivity to heavy products. From an applied point of view, in addition, these results, by confirming the presence of slight mass transfer restrictions which falsify the CO conversion kinetics on the eggshell sample, point out that engineered eggshell catalysts with an optimal thickness of the active shell represent an optimal solution to achieve high C_{15+} yields per mass of cobalt in the reactor, while limiting the ΔP in packed-bed reactors for the FTS. This is particularly relevant in view of the development of compact technologies to be used for the monetization of small and medium sized natural gas fields, as well as associated gas fields (flaring down projects). In those situations, indeed, it is crucial to limit the pressure drop in the reactor and to synthetize liquid products that can be easily transported far away from the natural gas source.

Acknowledgment

Sasol Germany GmbH is gratefully acknowledged for providing us with free Al_2O_3 samples.

Appendix A. Supplementary data

Supplementary data associated with this article can be found, in the online version, at http://dx.doi.org/10.1016/j.apcata.2015.12.011

References

[1] M. Dry, Handbook of Heterogeneous catalysis, in: H. Ertl, F. Knozinger (Eds.), second ed., Wiley-VCH, Weinheim, 2008, pp. 2965–2994.
[2] E. Iglesia, S.C. Reyes, R.J. Madon, S.L. Soled, Adv. Catal. 39 (1993) 221–302.
[3] C.G. Visconti, E. Tronconi, L. Lietti, R. Zennaro, P. Forzatti, Chem. Eng. Sci. 62 (2007) 5338–5343.
[4] C.G. Visconti, E. Tronconi, L. Lietti, P. Forzatti, S. Rossini, R. Zennaro, Top. Catal. 54 (2011) 786–800.
[5] C.G. Visconti, M. Mascellaro, Catal. Today 214 (2013) 61–73.
[6] C.G. Visconti, Ind. Eng. Chem. Res. 53 (2014) 1727–1734.
[7] Advances in Fischer–Tropsch Synthesis, Catalysts, and Catalysis, in: A. Jung, C. Kern, A. Jess, B.H. Davis, M.L. Occelli (Eds.), CRC, Press, Boca Raton, 2010, pp. 215–227.
[8] M.F.M. Post, A.C. Van't Hoog, J.K. Minderhoud, S.T. Sie, AIChE J. 35 (1989) 1107–1114.

[9] A.M. Hilmen, E. Bergene, O.A. Lindvag, D. Schanke, S. Eri, A. Holmen, Catal. Today 69 (2001) 227–232.
[10] F. Kapteijn, R.M. Deugd, J.A. Moulijn, Catal. Today 105 (2005) 350–356.
[11] C.G. Visconti, E. Tronconi, L. Lietti, G. Groppi, P. Forzatti, C. Cristiani, R. Zennaro, S. Rossini, Appl. Catal. A: Gen. 370 (2009) 93–101.
[12] C.G. Visconti, E. Tronconi, G. Groppi, L. Lietti, M. Iovane, S. Rossini, R. Zennaro, Chem. Eng. J. 171 (2011) 1294–1307.
[13] E. Iglesia, S.L. Soled, J.E. Baumgartner, S.C. Reyes, J. Catal. 153 (1995) 108–122.
[14] E. Peluso, C. Galarraga, H. De Lasa, Chem. Eng. Sci. 56 (2001) 1239–1245.
[15] Y.Q. Zhuang, M. Claeys, E. van Steen, Appl. Catal. A: Gen. 301 (2006) 138–142.
[16] J. Li, Y. Ding, X. Li, G. Jiao, T. Wang, W. Chen, H. Luo, Chem. Commun. 45 (2008) 5954–5955.
[17] C. Chen, H. Yuuda, X. Li, Appl. Catal. A: Gen. 396 (2011) 116–122.
[18] S.A. Gardezi, J.T. Wolan, B. Joseph, Appl. Catal. A: Gen. 447–448 (2012) 151–163.
[19] L. Fratalocchi, C.G. Visconti, L. Lietti, E. Tronconi, U. Cornaro, S. Rossini, Catal. Today 246 (2015) 125–132.
[20] R. Myrstad, S. Eri, P. Pfeifer, E. Rytter, A. Holmen, Catal. Today 147S (2009) S301–S304.
[21] A. Holmen, H.J. Venvik, R. Myrstad, J. Zhu, D. Chen, Catal. Today 216 (2013) 150–157.
[22] M. Iovane, R. Zennaro, P. Forzatti, G. Groppi, L. Lietti, E. Tronconi, C.G. Visconti, S. Rossini, E. Mignone, Patent Application WO/2010/130399, filed by Eni S.p.A. and Politecnico di Milano.
[23] D. Vervloet, F. Kapteijn, J. Nijenhuis, J. Ruud van Ommen, Catal. Today 216 (2013) 111–116.
[24] D. Schanke, S. Vada, E.A. Blekkan, A.M. Hilmen, A. Hoff, A. Holmen, J. Catal. 156 (1995) 85–95.
[25] G.L. Bezemer, J.H. Bitter, H.P.C.E. Kuipers, H. Oosterbeek, J.E. Holewijn, F. Xu, A.J. van Dillen, K.P. de Jong, J. Am. Chem. Soc. 128 (2006) 3956–3964.
[26] C.G. Visconti, L. Lietti, P. Forzatti, R. Zennaro, Appl. Catal. A: Gen. 330 (2007) 49–56.
[27] G. Jacobs, Y. Ji, B.H. Davis, D. Cronauer, A.J. Kropf, C.L. Marshall, Appl. Catal. A: Gen. 333 (2007) 177–191.
[28] F. Fiore, L. Lietti, G. Pederzani, E. Tronconi, R. Zennaro, P. Forzatti, Natural gas conversion VII, in: X. Bao, Y. Xu (Eds.), Studies in Surface Science and Catalysis, 147, Elsevier, Amsterdam, 2004.
[29] E. Iglesia, Appl. Catal. A: Gen. 161 (1997) 59–78.
[30] W. James, E.R. Becker, Catalysts for the control of automotive pollutants, in: J. McEvoy (Ed.), Advances in Chemistry, American Chemical Society, Washington, DC, 1975, pp. 116–132.
[31] R. Zennaro, M. Tagliabue, C.H. Bartholomew, Catal. Today 58 (2000) 309–319.